Solid-State ^{67}Zn NMR Spectroscopic Studies and ab Initio Molecular Orbital Calculations on a Synthetic Analogue of Carbonic Anhydrase

Andrew S. Lipton,[†] Catherine Bergquist,[‡] Gerard Parkin,*,[‡] and Paul D. Ellis*,[†]

Contribution from the Macromolecular Structure & Dynamics Directorate, WR Wiley Environmental Molecular Sciences Laboratory, Pacific Northwest National Laboratory, Richland, Washington 99352 and the Department of Chemistry, Columbia University, Mail Code 3115, 3000 Broadway, New York, New York 10027

Received November 4, 2002; E-mail: paul.ellis@pnl.gov

Abstract: The tris(pyrazolyl)hydroborato zinc complexes [Tp^{But,Me}]ZnX (where X = Br, Cl, and OH) have been examined by low-temperature solid-state ^{67}Zn NMR spectroscopy. The value of the quadrupole coupling constant, Cq, for the zinc increased monotonically with the electronegativity of the bound substituent X, e.g., Br < Cl ≪ OH. Calculations on the methylimidazole complex [(MeImH)$_3$Zn(OH)]$^+$ as a model for the active site of carbonic anhydrase indicate that the computed electric field gradient tensor is in good agreement with the experimental and calculated values for [Tp^{But,Me}]ZnOH.

Introduction

The principal motivation behind this research is the novel chemistry manifested by zinc and the associated biological significance of that chemistry. In zinc metalloproteins, the role of zinc can either be structural or catalytic. The structural role of zinc is dictated by its propensity to occupy tetrahedral sites rather than octahedral or pentacoordinate sites in metalloproteins. The catalytic properties often take advantage of the fact that the Zn^{2+} ion has an intermediate value of hardness or softness.[1] This intermediate hardness introduces an element of flexibility into the Lewis acidity of the Zn^{2+} ion. Several reviews on this aspect of zinc chemistry have been published.[1,2] One critical aspect of zinc chemistry of interest in bioinorganic chemistry involves the Zn−OH$_2$ functional group. Enzymes often use zinc to activate coordinated water toward deprotonation at close to neutral pH.

The Zn−OH$_2$ moiety is the principal catalytic functionality in the mechanism of action of the majority of zinc enzymes. For example, the conversion of the bound water to a hydroxide is central to the mechanism of action of carbonic anhydrase.[3] Depending upon the nature of the protein-derived ligands attached to the zinc, the water may require additional activation by interaction with the basic form of a proximal amino acid side chain. An additional type of activation relies upon the lability of the coordinated water to allow access of the substrate. Such a sequence is observed in the mechanism of action of liver alcohol dehydrogenase, in which an alcohol displaces coordinated water. Water is a critical component of most (if not all) catalytically active zinc sites in proteins and is activated by ionization, polarization, or poised for displacement depending upon the identity and spacing of the other coordinating ligands. This may be further augmented by other active-site residues, whose nature is responsible for detailed aspects of the mechanism of the catalytic reaction.[4] To understand how these mechanisms are determined, it is first absolutely essential to understand how the coordination environment modulates the chemistry of zinc.

Crystallography provides detailed 3-dimensional structures that cannot be deduced from spectroscopy. Crystallography is, of course, limited to crystalline samples. One niche for NMR spectroscopy is, thus, the structure determination for samples that have not been crystallized or for which reactive intermediates can be trapped at low temperature, but not in crystalline form. Exploitation of this niche is one of the prime motivations of the present research. However, even for crystalline samples, protein crystallography is often unable to provide high-accuracy structural detail for the metal site. In some cases, the metal site is disordered or partially occupied, even though the protein as a whole has a well-defined structure.[5,6] In other cases, protein crystallography simply has a large uncertainty, giving bond lengths and bond angles that are inconsistent with the known properties of the metal in small molecules.[6]

[†] Macromolecular Structure & Dynamics Directorate, WR Wiley Environmental Molecular Sciences Laboratory, Pacific Northwest National Laboratory.

[‡] Department of Chemistry, Columbia University.

(1) Frausto da Silva, J. J. R.; Williams, R. J. P. *The Biological Chemistry of the Elements. The Inorganic Chemistry of Life*; Clarendon Press: Oxford, Oxford University Press: New York, 1991; Lippard, S. J.; Berg, J. M., *Principles of Bioinorganic Chemistry*; University Science Books: Mill Valley, California; 1994; Lipscomb, W. N.; Sträter, N. *Chem. Rev.* **1996**, *96*, 2375.

(2) Parkin, G. *Chem. Commun.* **2000**, 1971. (b) Parkin, G. *Met. Ions Biol. Syst.*; Sigel, A., Sigel, H., Eds.; M. Dekker: New York, 2001; Vol. 38, Chapter 14, pp 411−460;.

(3) Christianson, D. W. and Fierke, C. A. *Acc. Chem. Res.* **1996**, *29*, 331−339.

(4) Vallee, B. L.; Auld, D. S. *Proc. Natl. Acad. Sci., U. S. A.* **1990**, *87*, 220−224.

(5) Rosenzweig, A. C.; Huffman, D. L.; Hou, H. Y.; Wernimont, A. K.; Pufahl, R. A.; O'Halloran, T. V. *Structure* **1999**, *7*, 605−617.

(6) Alberts, I. L.; Nadassy, K.; Wodak, S. J. *Protein Sci.* **1998**, *7*, 1700−1716.

A long-term goal of this research is to obtain a thorough understanding of the bioinorganic chemistry of zinc by investigating proteins and their synthetic analogues that are designed to mimic both the structure and function of the active sites of zinc enzymes. One of the vehicles to obtaining this objective is through the use of spectroscopy. Unfortunately, with a stable $3d^{10}$ electron configuration, the Zn^{2+} ion is not amenable to investigation by either UV−vis or EPR spectroscopy. However, it has recently been demonstrated that solid-state ^{67}Zn NMR can be made practical by utilizing cross-polarization[7] (CP) methods in combination with low temperature (<25 K) and paramagnetic dopants.[8,9,10] It is essential to characterize the sensitivity of ^{67}Zn NMR parameters (quadrupole coupling, Cq, and chemical shielding, σ, tensors and their relative orientations) to subtle changes of structure in order to be able to relate these changes to specific structural/electronic effects. As an illustration of the sensitivity of ^{67}Zn NMR parameters to coordination number, symmetry, and structure, we previously examined the homoleptic 4- and 6-coordinate zinc(II) poly(pyrazolyl)borate complexes, [$H_2B(pz)_2]_2Zn$, [$H_2B(3,5-Me_2pz)_2]_2Zn$, [$HB(pz)_3]_2Zn$, and [$HB(3,5-Me_2pz)_3]_2Zn$, where pz denotes a pyrazolyl ring.[10] Although these investigations were informative, the zinc centers in these complexes, with tetrahedral [ZnN_4] and octahedral [ZnN_6] coordination, bear little resemblance to the tetrahedral [ZnN_3O] motif of the active site of carbonic anhydrase.

Therefore, in this paper, we report solid-state ^{67}Zn NMR spectroscopic studies on a more representative synthetic analogue of carbonic anhydrase, namely the tris(3-*tert*-butyl-5-methylpyrazolyl)hydroborato zinc complex [$Tp^{But,Me}$]ZnOH[11] which not only possesses the requisite [ZnN_3O] motif, but also reacts with CO_2 to generate a bicarbonate complex.[12] Furthermore, studies on the halide derivatives [$Tp^{But,Me}$]ZnX (X = Br, Cl) have been carried out to determine the impact of a zinc substituent on the derived NMR spectroscopic parameters.

Experimental Section

Synthesis. Preparation of Co^{II} doped [Tp^{But,Me}]ZnX. All manipulations were performed under a N_2 atmosphere employing standard Schlenk and glovebox techniques. [$Tp^{But,Me}$]ZnOH[12] and [$Tp^{But,Me}$]CoI[13] were prepared as previously reported, while [$Tp^{But,Me}$]ZnX (X = Br, Cl) were prepared by methods analogous to [Tp^{But}]ZnX.[14] Samples of [$Tp^{But,Me}$]ZnX doped with ca. 2 wt % of [$Tp^{But,Me}$]CoI were prepared by a sequence involving dissolving the mixture in benzene, followed by lyophilization to remove the benzene and give a amorphous solid mixture of [$Tp^{But,Me}$]ZnX and [$Tp^{But,Me}$]CoI. All samples were prepared using isotopically normal zinc (4.11%).

^{67}Zn NMR Spectroscopy. All of the ^{67}Zn (4.11%) NMR experiments were performed obtained at 10 K using a home-built probe[8] in an Oxford cryostat and a Varian Infinity^{Plus} console in combination with Miteq cryogenic preamplifier. The pulse sequence utilized was a combination of CP[7] and a train of CPMG[15] spin−echoes, or the CP/QCPMG

Table 1. Observed and Optimized Geometries

	[Tp^{But,Me}] ZnOH X-ray	[Tp^{But,Me}] ZnOH RHF	[Tp^{But,Me}] ZnOH DFT	[(MeImH)$_3$ ZnOH]$^+$RHF
$\langle R_{Zn-N}\rangle$ (Å)	2.052	2.111	2.086	2.099
R_{Zn-O} (Å)	1.850	1.858	1.864	1.867
R_{O-H} (Å)	a	0.938	0.960	0.938
$\angle_{ZnOH}$ (°)	a	122.57	116.39	123.90

^{a} The hydrogen atom of the OH group was not determined in the crystal structure.

pulse sequence.[8] Typical values for the experimental parameters used are ^1H $\pi/2$ pulse duration of 3.6 μs, a selective ^{67}Zn π pulse width of 3.25 μs, and a spectral width of 1 MHz. Each lineshape was reconstructed from multiple data sets which were shifted in frequency to account for the excitation bandwidth of the CP.[10] Recycle delays for each experiment (and sample) were 5 s with the number of acquisitions per block being 1024, 4096, and 4096 for the Br, Cl and OH, respectively. All ^{67}Zn chemical shifts are referenced to a 0.5 M aqueous solution of zinc acetate at room temperature. The quadrupole tensors were extracted from the lineshapes using a combination of an in-house program and the program SIMPSON.[16] The relative uncertainty in quadrupole coupling constant, Cq, is ± 0.1 MHz and the asymmetry parameter is 0.05.

Ab Initio Calculations. The calculations of the electric field gradient (EFG) tensors were performed using the Gaussian 98 suite of programs.[17] The geometry of [$Tp^{But,Me}$]ZnOH determined by X-ray crystallography[11] was used as an initial structure except for the addition of the hydroxyl proton. This atom was added with R_{OH} = 1.030 Å and $\angle_{ZnOH}$ = 109.47°. The structure was optimized using restricted Hartree−Fock (RHF) and density functional theory (DFT) methods. In the DFT calculations the B3LYP method was employed.[17] The experimental and calculated structures are compared in Table 1. The EFG tensor was then computed using the optimized geometries with RHF, DFT and MP2 (with the RHF structure). An idealized model was also constructed using methyl groups on the imidazole rings to distinguish between the nitrogens of the ring thus making it more closely resemble the side chain of a histidine. The nitrogen nearest to the methyl is N_δ and the other is N_ϵ. The nitrogens are coordinated to H or Zn. To resemble the active site of CA the zinc is coordinated by one δ- and two ϵ-nitrogens and a hydroxide ligand.[3,18] This structure was also optimized at the RHF level and the EFG tensor calculated. Depicted in Figure 1 is a schematic of the nomenclature of the nitrogens of the methylimidazole and the geometry optimized structure.

The triple-ξ level (including polarization functions) basis set of Ahlrichs[19] was used for all calculations. The basis set for zinc was further augmented with a single p-, and d-function, and a pair of f-functions using the program g98opt.[17] The coefficients derived from these calculations can be found at the end of ref 19. The density matrix used for the calculation of the field gradient calculations was computed after the scf portion of the calculation had converged to an RMS level of 10^{-8} or better. The calculations were carried out on an 8 CPU Silicon Graphics Origin 2000 Computer.

(7) Pines, A.; Gibby, M. G., Waugh, J. S. *J. Chem. Phys.* **1972**, *56*, 1776.
(8) Lipton, A. S.; Sears, J. A.; Ellis, P. D. *J. Magn. Reson.* **2001**, *151*, 48.
(9) Lipton, A. S.; Buchko, G. W.; Sears, J. A.; Kennedy, M. A.; Ellis, P. D. *J. Am. Chem. Soc.* **2001**, *123*, 992−993.
(10) Lipton, A. S.; Wright, T. A.; Bowman, M. K.; Reger, D. L.; Ellis, P. D. *J. Am. Chem. Soc.* **2002**, *124*, 5850−5860.
(11) Alsfasser, R.; Trofimenko, S.; Looney, A.; Parkin, G.; Vahrenkamp, H. *Inorg. Chem.* **1991**, *30*, 4098−4100.
(12) Looney, A.; Han, R.; McNeill, K.; Parkin, G. *J. Am. Chem. Soc.* **1993**, *115*, 4690−4697.
(13) Egan, J. W., Jr.; Haggerty, B. S.; Rheingold, A. L.; Sendlinger, S. C.; Theopold, K. H. *J. Am. Chem. Soc.* **1990**, *112*, 2445−2446.
(14) Yoon, K.; Parkin, G. *J. Am. Chem. Soc.* **1991**, *113*, 8414−8418.
(15) Carr, H. Y.; Purcell, E. M. *Phys. Rev.* **1954**, *94*, 630. (b) Meiboom, S.; Gill, D. *Rev. Sci. Instrum.* **1958**, *29*, 688.

(16) Bak, M.; Rasmussen, J. T.; Nielsen, N. C. *J. Magn. Reson.* **2000**, *147*, 296.
(17) Frisch, M. J.; Trucks, G. W.; Schlegel, H. B.; Scuseria, G. E.; Robb, M. A.; Cheeseman, J. R.; Zakrzewski, V. G.; Montgomery, J. A., Jr.; Stratmann, R. E.; Burant, J. C.; Dapprich, S.; Millam, J. M.; Daniels, A. D.; Kudin, K. N.; Strain, M. C.; Farkas, O.; Tomasi, J.; Barone, V.; Cossi, M.; Cammi, R.; Mennucci, B.; Pomelli, C.; Adamo, C.; Clifford, S.; Ochterski, J.; Petersson, G. A.; Ayala, P. Y.; Cui, Q.; Morokuma, K.; Malick, D. K.; Rabuck, A. D.; Raghavachari, K.; Foresman, J. B.; Cioslowski, J.; Ortiz, J. V.; Stefanov, B. B.; Liu, G.; Liashenko, A.; Piskorz, P.; Komaromi, I.; Gomperts, R.; Martin, R. L.; Fox, D. J.; Keith, T.; Al-Laham, M. A.; Peng, C. Y.; Nanayakkara, A.; Gonzalez, C.; Challacombe, M.; Gill, P. M. W.; Johnson, B. G.; Chen, W.; Wong, M. W.; Andres, J. L.; Head-Gordon, M.; Replogle, E. S.; Pople, J. A. *Gaussian 98*, revision A.7; Gaussian, Inc.: Pittsburgh, PA, 1998.
(18) Lippard, S. J.; Berg, J. M. In *Principles of Bioinorganic Chemistry*; Kelly, A., Ed.; University Science Books: Mill Valley, CA, 1994; pp 267−271.
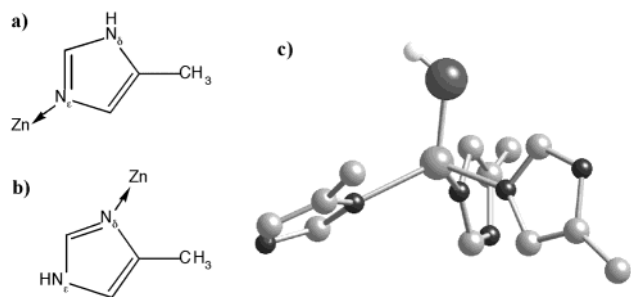
Figure 1. (a) and (b) Illustration of two isomeric forms of methylimidazole coordinated to zinc in [(MeImH)$_3$ZnOH]$^+$, and (c) the optimized geometry of [(MeImH)$_3$ZnOH]$^+$.

Table 2. Extracted Parameters from the Solid-State NMR Lineshapes

parameters[a]	[Tp$^{Bu^t,Me}$] ZnBr	[Tp$^{Bu^t,Me}$] ZnCl	[Tp$^{Bu^t,Me}$] ZnOH
σ_{iso} (ppm)[b]	57.7	311.3	166.5
Cq (MHz)	9.5	12.3	30.5
η_q[4]	0	0	0
$\Delta\sigma$ (ppm)	−374.9	−243.1	−301.2

[a] $\sigma_{iso} = (\sigma_{11} + \sigma_{22} + \sigma_{33})/3$; $\Delta\sigma = \sigma_{33} - (\sigma_{11} + \sigma_{22})/2$; $|\sigma_{iso}\text{-}\sigma_{33}| > |\sigma_{iso}\text{-}\sigma_{11}| > |\sigma_{iso}\text{-}\sigma_{22}|$. [b] Chemical shift is referenced to 0.5 M zinc acetate at room temperature. [c] The asymmetry parameter, η_q, as well as η_σ and the Euler angles between the quadrupole and shielding PAS frames were restricted to 0 during the optimizations.

Results and Discussion

The quadrupole and chemical shift parameters for [Tp$^{Bu^t,Me}$]-ZnOH, [Tp$^{Bu^t,Me}$]ZnBr, [Tp$^{Bu^t,Me}$]ZnCl are summarized in Table 2. Due to the near axial symmetry of the spectra, the asymmetry parameter, η, was restricted to 0 in the simulations and the PAS frame for the shielding interaction was held to be coincident with the EFG frame when included. The experimental and simulated data are depicted in Figure 2. In each case the inclusion of chemical shielding anisotropy (CSA) was necessary to correctly place the "magic angle" feature of the lineshape. However the lineshapes are dominated by the second-order quadrupole interaction.

An approximate view of the quadrupole coupling constant has been provided by Slichter.[20] In this treatment, the V_{zz} element of the field gradient (and therefore Cq) is directly proportional to $1/r^3$ and the electronic charge distribution. This relation results in the sensitivity of Cq to the charge at the nucleus of interest and that of directly bonded neighbors. Hence, Cq should be reflective of those parameters that describe the nature of the bonding to the atomic center of interest. However, for spherically symmetric charges (i.e., *s*-orbitals or closed shell) there is no contribution to the quadrupole coupling. Therefore, the quadrupole coupling for the *s*-part of a hybridized bond or ionic bonding vanishes. This implies Cq can be utilized to study bond hybridization or degree of covalency.[21]

(19) Basis sets were obtained from the Extensible Computational Chemistry Environment Basis Set Database, Version 1/29/01, as developed and distributed by the Molecular Science Computing Facility, Environmental and Molecular Sciences Laboratory which is part of the Pacific Northwest Laboratory, P. O. Box 999, Richland, WA 99352, USA, and funded by the U.S. Department of Energy. The Pacific Northwest Laboratory is a multi-program laboratory operated by Battelle Memorial Institute for the U.S. Department of Energy under contract DE-AC06−76RLO 1830. Contact David Feller or Karen Schuchardt for further information. The augmented values of the coefficients are: p: 0.1624500; d: 0.1104370; f: 1.443255456 and 0.158697540.
(20) Slichter, C. P. *Principles of Magnetic Resonance*, 3rd ed.; Springer-Verlag: New York; 1978, 1990; Ch 10.
(21) Dailey, B. P.; Townes, C. H. *J. Chem. Phys.* **1955**, *23*, 118.

Assuming the [Tp$^{Bu^t,Me}$]-Zn framework is similar for [Tp$^{Bu^t,Me}$]-ZnOH, [Tp$^{Bu^t,Me}$]ZnBr, and [Tp$^{Bu^t,Me}$]ZnCl, the changes observed in Cq are due to the contributions from the bromide, chloride and hydroxide ligands. As one would intuitively expect, the quadrupole coupling or Cq increases with electronegativity Br (2.8) < Cl (3.0) < O (3.5).[22] The Cq is also sensitive to the Zn-X distance (single bond covalent radii of Br:1.14 Å, Cl:0.99 Å, and O:0.74 Å).[22] As the hydroxide species represents the largest ^{67}Zn quadrupole coupling reported to date, the question becomes why is this so dramatic a change from other zinc species studied? Since the changed in the electronegativities of the ligands can be viewed as incremental, one can conclude that the large change in Cq is more reflective of the shorter Zn−O bond than the electronic consequences of the changes in electronegativity.

To determine if this large Cq is understandable, we have performed ab initio molecular orbital calculations on [Tp$^{Bu^t,Me}$]-ZnOH to compare its predicted field gradient tensor with its experimental value and also compare the values with that of a proposed model for the active site of carbonic anhydrase, namely [(MeImH)$_3$Zn(OH)]$^+$. Both structures are monomeric and devoid of hydrogen bonding and, as such, do not have the added complication that those electrostatics could potentially introduce. This is in contrast to polymeric systems, such as zinc formate or zinc diacetate dihydrate, which have extensive hydrogen bonding networks and give poor results for field gradient calculations unless several unit cells are included in the calculation. The limiting factor in our ability to predict Cq here is the quality of the basis sets used. The quadrupole coupling constant, Cq, is given by

$$Cq = q_{zz}[e^2/(a_0^3 h)]Q \tag{1}$$

where Q is the quadrupole moment of the nucleus in question, and q_{zz} is the *zz* element of the field gradient tensor. The atomic constants (*e*, a_0, and *h*) have their usual meanings. Utilizing the value of Q for ^{67}Zn of 0.15×10^{-24} cm^2 from Harris and Mann[23] we are left with

$$Cq = q_{zz}\cdot35.24473 \text{ MHz} \tag{2}$$

The conventions defining q_{zz} and the asymmetry parameter, η_q, are as follows[24]

$$|q_{zz}| \geq |q_{xx}| \geq |q_{yy}| \tag{3}$$

and

$$\eta_q = (q_{yy} - q_{xx})/q_{zz} \tag{4}$$

Cq was calculated for the optimized structures described above, as summarized in Table 3. The Cq for the RHF geometry optimized structure of [Tp$^{Bu^t,Me}$]ZnOH is calculated to be 37.73 (34.37 MHz for the MP2 calculation), which is greater than the experimentally measured value of 30.51 MHz. Furthermore,

(22) Pauling, L. *The Nature of The Chemical Bond*, 3rd ed.; Cornell University Press: Ithaca, New York, 1960.
(23) Harris, R. K. Introduction. In *NMR and the Periodic Table*; Harris, R. K., Mann, B. E., Eds.; Academic Press: New York, 1978; 1−19.
(24) Spiess, H. W. Rotation of Molecules and Nuclear Spin Relaxation. In *NMR Basic Principles and Progress*; Diehl, P., Fluck, E., Kosfeld, R., Eds.; Springer; New York, 1978; Vol 15, 55−214.
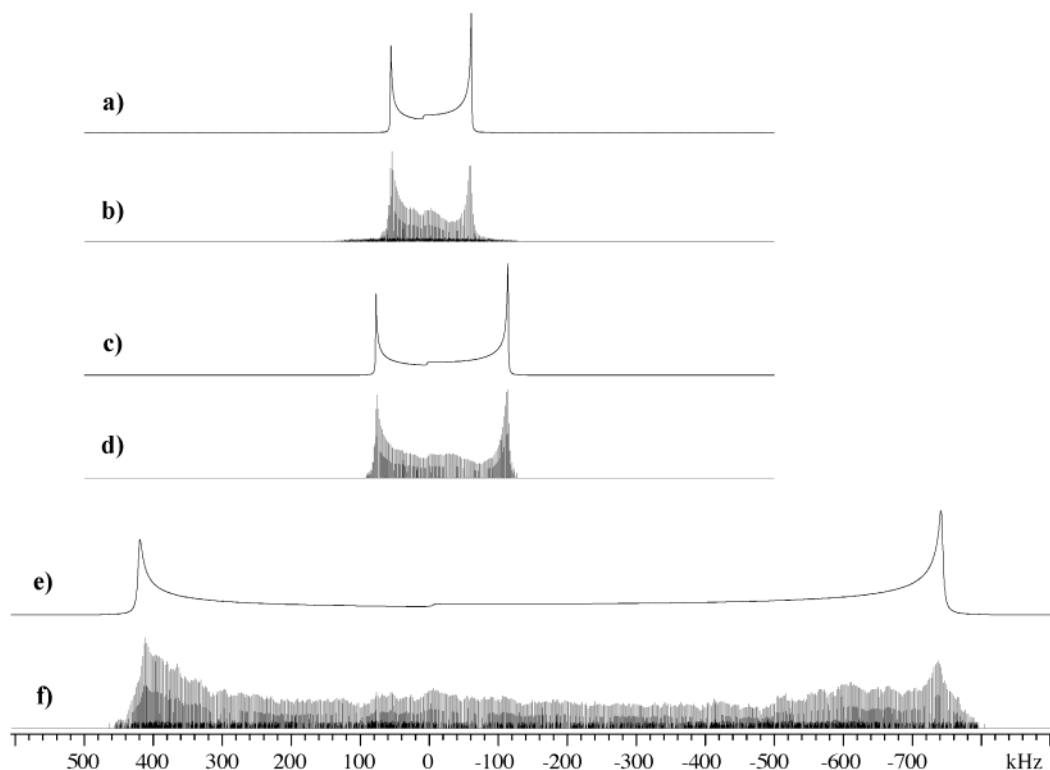
Figure 2. Simulated and experimental ^{67}Zn NMR data for [Tp^{But,Me}]ZnX, where X denotes (a, b) Br, (c, d) Cl, and (e, f) OH at 9.4 T and 10 K.

Table 3. Predicted Electric Field Gradients

	[Tp^{But,Me}]ZnOH (RHF geometry)	[Tp^{But,Me}]ZnOH (DFT geometry)	[(MeImH)$_3$ZnOH]$^+$ (RHF geometry)
V_{zz}	1.0704 (0.9751)^a	0.8114	0.8285
Cq (MHz)	37.7 (34.4)^a	28.6	29.2

^{a} Single point MP2 calculation using the RHF optimized geometry.

a calculation on the DFT geometry optimized structure gave a value of 28.60 MHz. The experimentally determined value is thus within the range of the calculated values.

The average Zn−N distance computed for the model [(MeImH)$_3$Zn(OH)]$^+$ was found to be 2.098 Å with a Zn−O distance of 1.867 Å using restricted Hartree−Fock methods. The value of Cq predicted is 29.2 MHz, which is in good agreement both with the predicted and experimental values for [Tp^{But,Me}]ZnOH. The simulated lineshapes from these predicted Cq's are depicted in Figure 3. All the asymmetry parameters have been restricted to 0.0 for easier comparison with the experimental data (shown in Figure 3e).

Conclusions

Previous natural abundance ^{67}Zn experiments have been limited to models or proteins with Cq values that are less than 15 MHz. We have shown here that using our methodology it is possible to acquire the ^{67}Zn solid-state NMR spectrum from a natural abundance (^{67}Zn is 4.11% abundant) complex with a large Cq (>30 MHz) value. The baseline-to-baseline width of the line shape for a given value of the asymmetry parameter is proportional to Cq^2. It is doubtful that one could have observed a resonance spread over 1.3 MHz via standard room-temperature CP experiments. Similarly, it is reasonable to conclude that any protein experiments with similar Cq values (due to the increased
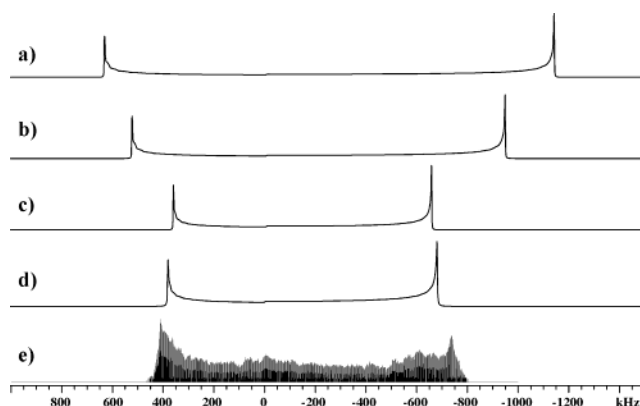

Figure 3. Predicted 9.4 T ^{67}Zn NMR spectra from ab initio MO theory contrasted with the experimental spectrum of [Tp^{But,Me}]ZnOH where; (a) is from a fully RHF optimized geometry, (b) used the optimized RHF geometry and a single point MP2 calculation, (c) used a DFT optimized geometry, (d) is from an RHF optimized geometry on [(MeImH)$_3$ZnOH]$^+$, and (e) is the experimental spectrum of [Tp^{But,Me}]ZnOH.

dilution of the metal) could not be performed at room temperature.

The complete data set for [Tp^{But,Me}]ZnOH was acquired in 44 blocks, moving the transmitter every 30 kHz for a total of approximately 10.5 days of experiment time. With enrichment (currently only 88% ^{67}Zn is commercially available) one could observe an equal amount of an 11 kDa protein with a 30 MHz Cq in the same amount of time. However, there are other improvements which can be made such as multiple contact CP (providing between 70% to 90% additional signal) and changing the spikelet spacing (increasing the spikelet separation from 2 kHz to 4 kHz will double the signal-to-noise ratio) that allow the observable molecular weight to be increased to that of CA or larger proteins. Additionally, if the electric field gradient at

the Zn^{2+} of interest in a hypothetical protein gives rise to a smaller value of Cq, the level of difficulty of the experiment decreases quadratically as the ratio of the Cq's. This value of 30 MHz for Cq is currently the largest in the literature for ^{67}Zn measured by NMR and does not appear to represent a limit to the capabilities of this methodology to follow the varied structural topology at Zn^{2+}.

Further, we have shown that ^{67}Zn solid-state NMR parameters (Cq) are sensitive to changes in the coordination environment. Likewise we have determined that a synthetic analogue of the high pH form of a protein such as CA or insulin (which has a similar coordination environment) should have a Cq of roughly 30 MHz. This was verified by creating a hypothetical complex that mimics the active site of carbonic anhydrase, $[(MeImH)_3Zn\text{-}(OH)]^+$, and calculating its Cq. The main assumption is that the electrostatics associated with hydrogen bonding to the water network in the active site and to the side chains of the histidines coordinated to the metal of the protein do not significantly impact the observed field gradient.